Multiple antidiabetic effects of three α-glucosidase inhibitory peptides, PFP, YPL and YPG: Dipeptidyl peptidase–IV inhibition, suppression of lipid accumulation in differentiated 3T3-L1 adipocytes and scavenging activity on methylglyoxal

Mohammed Auwal Ibrahim[a,c*], June C. Serem[b], Megan J. Bester[b], Albert W. Neitz[a] and Anabella R.M. Gaspar[a]

[a]Department of Biochemistry, Genetics and Microbiology, University of Pretoria, Pretoria 0002, South Africa
[b]Department of Anatomy, University of Pretoria, Pretoria 002, South Africa
[c]Department of Biochemistry, Ahmadu Bello University, Zaria, Nigeria

***Correspondence to:** Dr. Mohammed Auwal Ibrahim, Department of Biochemistry, Genetics and Microbiology, Faculty of Natural and Agricultural Sciences, University of Pretoria, Pretoria 0002, South Africa E mail: mauwalibrahim@gmail.com or maibrahim@abu.edu.ng

Highlights

• The peptides PFP, YPL and YPG were investigated for multiple antidiabetic effects.

• *In vitro*, the peptides inhibited dipeptidyl peptidase-4 but YPG was the best.

• YPG was the best in preventing lipid accumulation in 3T3-L1 differentiated adipocytes.

• Along with other parameters, YPG is the best multifunctional antidiabetic candidate.

ABSTRACT

Antidiabetic agents with multiple targets have the greatest pharmaceutical potential. In this study, three α-glucosidase inhibitory peptides, PFP, YPL and YPG, were investigated for additional antidiabetic targets viz; dipeptidyl peptidase-IV inhibition (DPP-IV), lipid accumulation and the differentiation of 3T3-L1 adipocytes, and scavenging of methylglyoxal (MGO), reactive oxygen species (ROS) and nitric oxide (NO). The peptides were subjected to molecular docking on human DPP-IV where the binding free energies were PFP < YPG < YPL < diprotin A while hydrogen bond interactions were critical in the binding of YPL and YPG. Moreover, YPG demonstrated significantly higher ($p<0.05$) *in vitro* DPP-IV inhibition than PFP and YPL. Kinetic analysis revealed that all three peptides are uncompetitive inhibitors of DPP-IV while YPG had the lowest inhibition binding constant. PFP and YPG prevented lipid accumulation in 3T3-L1 differentiated adipocytes but may be due to cytotoxicity for PFP. The peptides scavenged MGO, ROS and NO but only the ROS and NO scavenging activities of YPG were comparable to glutathione. In conclusion, PFP, YPL and YPG exhibited DPP-IV inhibitory activity, reduced adipocyte differentiation and lipid accumulation as well as scavenged MGO, ROS and NO. However, YPG had the best potential as a possible multifunctional antidiabetic agent.

Key words*:* Adipocytes differentiation; Antioxidant activity; Dipeptidyl peptidase IV inhibition; α-Glucosidase inhibitory peptides; Methylglyoxal; Molecular docking,

1. Introduction

Type 2 diabetes mellitus (T2DM) is currently one of the fastest growing public health concerns affecting both the developed and developing world. It is metabolic derangement characterized by hyperglycemia as a result of deficiency in insulin action which consequently affects carbohydrate, lipid and protein metabolism [1]. Dysfunction of the differentiation of adipocytes causes lipodystrophy associated with impaired glucose and lipid homeostasis [2] while increased levels of oxidative stress and non-enzymatic glycation is a major cause of vascular damage leading to associated pathologies. Due to T2DM being a multifaceted disease, multiple therapeutic strategies are exploited in its management [3]. Consequently, several classes of antidiabetic drugs have been developed which include sulfonylureas, biguanides, thiazolidinediones, sodium-glucose cotransporter 2 inhibitors, gliptins, α-glucosidase inhibitors among others [4]. Most of these antidiabetic drugs have side effects which often limit their therapeutic benefits [4]. Hence, the search for novel antidiabetic agents with fewer side effects and multiple antidiabetic targets is essential.

Bioactive peptides are specific fragments of proteins that modulate physiological functions through interactions with specific receptors and consequently induce a physiological response leading to beneficial health effects [5]. These peptides have recently attracted scientific attention as components of functional foods due to low allergenicity and multifunctional properties which include antimicrobial [6], antioxidant [7], antihypertensive [8], anticancer [9] and antithrombotic [10] effects. More relevant to the treatment of T2DM, a number of bioactive peptides have antidiabetic effects by inhibiting α-glucosidase activity [11] and stimulating insulin-mediated glucose uptake [12]. Indeed, with respect to α-glucosidase inhibition, we recently reported the identification of 43 fully sequenced α-glucosidase inhibitory peptides [11] which includes 4 tripeptides; PFP, YPY, YPL and YPG. However, a characteristic of many bioactive peptides is the multifunctional properties. For the treatment of T2DM, an ideal multifunctional peptide inhibits several enzymatic T2DM targets, reduces oxidative stress, methylglyoxal mediated glycation and restores lipid homeostasis.

Dipeptidyl peptidase-IV (DPP-IV; EC3.4.14.5) is a serine protease that rapidly hydrolyses the incretin hormones which include glucose-dependent insulinotropic polypeptide and glucagon-like peptide-1. Increasing the half-lives of these incretins by the inhibition of DPP-IV,

increase insulin secretion, and decrease gastric emptying and blood glucose levels. Thus, DPP-IV inhibition is a promising pharmaceutical approach currently exploited for the management of diabetes [13]. In addition to altering glucose homeostasis, T2DM is associated with increased levels of cholesterol and triacylglycerols which are implicated in the development of atherosclerosis and considered to be an important macrovascular complication associated with the disease [14]. Therefore, the control of these lipid levels and accumulation is a major therapeutic goal of T2DM. The differentiated 3T3-L1 fibroblast model is a well-established cell line that has been pivotal in advancing the understanding of basic cellular mechanisms associated with adipogenesis [15]. This cell line is therefore a suitable model for studying lipid accumulation and effects of drugs on lipid homoestasis especially considering the role of adipocytes in the development of T2DM [15, 16].

Another important mechanism of pathogenesis for T2DM is increased oxidative stress [14] and accumulation of methylglyoxal (MGO) which causes advanced glycated end products (AGEs) that are known to contribute to T2DM-associated complications. Oxidative stress, an imbalance between oxidants and antioxidants in the body is the result of hyperglycemia-induced mitochondrial superoxide overproduction [14] which leads to the generation of potent reactive oxygen species (ROS) and reactive nitrogen species (RNS) when it reacts with oxygen-based radicals and nitric oxide (NO), respectively [17]. Indeed, the crucial role of NO to most aspects of diabetes and the associated complications has been extensively reviewed [17]. On the other hand, a growing body of evidence has suggested that, in T2DM, oxidative stress and reduced activity of glyoxylase 1 are mainly responsible for accumulation of MGO which has many intra- and extracellular targets with numerous deleterious effects including cell death, inflammation, impaired angiogenesis and macrovascular complications [18]. Recently, Moraru et al. [19] demonstrated that elevated MGO levels contribute significantly to several aspects of T2DM pathogenesis including insulin resistance, obesity and hyperglycemia which suggests preventing the accumulation of this reactive metabolite is a beneficial therapeutic option against T2DM. Based on the foregoing, it is evident that patients with T2DM could immensely benefit from the development of any pharmaceutical product with scavenging effects toward oxygen-based and nitric oxide radicals in addition to reducing the levels of MGO.

In this study, additional beneficial antidiabetic effects of tripeptides, PFP, YPL and YPG with α-glucosidase inhibitory activity were evaluated. These include *in silico* and *in vitro* DPP IV inhibitory activity, the effect of these peptides on lipid accumulation in differentiating and differentiated 3T3-L1 cells as well as the ability of these peptides to scavenge MGO, ROS and NO.

2. Materials and methods

2.1 Chemicals and reagents

Kidney DPP-IV, Gly-Pro-p-nitroanilide, diprotin A isobutylmethylxanthine (IBMX), dexamethasone, insulin, Dulbecco's modified Eagle's medium (DMEM), rosiglitazone, methylglyoxal, bovine serum albumin (BSA), fluorescein, 2,2' -azobis(2-amidinopropane) dihydrochloride (AAPH), reduced glutathione (GSH), antibiotic solution (10000 units penicillin, 10 mg streptomycin, 25 μg amphotericin B per mL) and Oil Red O were from Sigma-Aldrich Chemical Company (Johannesburg, South Africa (SA)). Dimethylsulfoxide (DMSO), sodium nitroprusside, sulphanilamide, trypsin, N-(1-Naphthyl)-ethylenediamine-dihydrochloride (NED), 3-[4,5-dimethylthiazol-2-yl]-2,5-diphenyltetrazolium bromide (MTT) were obtained from Merck (Johannesburg, SA) while foetal calf serum (FCS) was obtained from Capricon Scientific (GmBH, Germany). The peptides PFP, YPL and YPG were procured from Genscript (New Jersey, USA).

2.2 Molecular docking studies

The three tripeptides were subjected to molecular docking to determine *in silico* inhibitory potential towards human DPP-IV. To perform the molecular docking analysis, the 3D crystal structures of the human DPP-IV (PDB ID 1WCY resolved to 2.20Å by x-ray diffraction) was retrieved in PDB format from the protein data bank (www.rcsb.org). Subsequently, chimera version 1.11.2 (www.cgl.ucsf.edu/chimera/) was used to remove the co-crystallized ligand and water molecules from the protein structure. Thereafter, the dock prep tool of the chimera software was used to prepare the protein for docking. All default parameters for the dock prep tool in chimera were used. The PDB prepared versions of the protein and the peptide ligands were opened in chimera and subjected to the Autodock Vina tool [20] in the same software. The grid sizes (xyz points) were set as 59.3051, 60.8384 and 41.5917 while the grid centers were

designated at dimensions (x, y and z) 43.7338, 47.5112 and 66.0177. Other parameters of Autodock Vina in chimera were left as default. AutoDock Vina employs iterated local search global optimizer and all output files were saved in pdbqt format. After the successful docking, the minimum binding free energy for each of the peptides was recorded while the docking pose was extracted and aligned with the receptor structure for further analysis of hydrogen bond interactions.

2.3 Peptide synthesis and preparation

The three peptides PFP, YPL and YPG were synthesized by Flexpeptide^{TM} technology by GenScript. The purity, molecular mass and amino acid analysis of the peptides were determined by the manufacturer using reverse phase high performance liquid chromatography and mass spectrometry. Stock peptide solutions were prepared in sterile deionized double distilled water.

2.4 α-Glucosidase inhibitory activity of the peptides

Prior to other studies, it was necessary to confirm the reported α-glucosidase inhibitory activity of the three peptides in our laboratory. The reaction of yeast α-glucosidase with pNPG as substrate is the most widely used assay for this purpose. Indeed, 39 out of the 43 fully sequenced α-glucosidase inhibitory peptides reported in the literature were investigated using this reaction [11]. Therefore, for comparative and verification purposes, the same reaction was used to validate the previously reported IC_{50} values of the peptides against α-glucosidase [11, 21, 22]. The inhibitory activity was assayed according to a previously described method with slight modifications. Briefly, 50 µL of each peptide or acarbose at a final concentration of 15.63-500 µM was incubated with 25 µL of 0.5 U/mL α-glucosidase solution in 100 mM phosphate buffer (pH 6.8) at 37 ^{o}C for 60 min. Thereafter, 25 µL of a 5 mM pNPG solution in 100 mM phosphate buffer (pH 6.8) was added and the mixture was further incubated at 37 ^{o}C for 30 min. The absorbance of the released *p*-nitrophenol was measured at 405 nm using Spectramax paradigm multi-mode microplate reader (Molecular Devices LLC, USA) and the inhibitory activity was expressed as percentage of a control sample without the inhibitors. The α-glucosidase inhibitory activity of the peptides was calculated by using the following formula:

$$\alpha - \text{Glucosidase inhibitory activity } (\%) = \left(1 - \frac{\text{As}}{\text{Ac}}\right) \text{x } 100$$

where As and Ac are absorbance of sample and absorbance of control respectively. The concentrations of the peptides resulting in 50% inhibition of enzyme activity (IC_{50} values) were determined using the straight-line equations of the percentage inhibitory activity against the respective logarithm of peptide concentrations [24].

2.5 DPP-IV inhibitory activity of the peptides

The DPP-IV inhibitory activity of the peptides was determined using the method described by Konrad et al. [25]. Briefly, 50 µL of the peptides at final concentrations of 31.25-500 µM was incubated with 25 µL 0.02 U/mL DPP-IV re-suspended in 100 mM Tris-HCl buffer (pH 8.0) at 37 ^{o}C for 60 min. Thereafter, 25 µL of 6 mM Gly-Pro-*p*-nitroanilide was added to the reaction mixture and further incubated at 37 ^{o}C for 60 min. The absorbance of the released *p*-nitroanilide was measured at 405 nm using Spectramax paradigm multi-mode microplate reader (Molecular Devices LLC, USA) and the inhibitory activity was expressed as percentage of a control sample without the inhibitors. A standard DPP-IV inhibitor, diprotin A, was also similarly treated and served as a positive control. The DPPIV inhibitory activity of the peptides was calculated by using the following formula:

$$\text{DPP} - \text{IV inhibitory activity } (\%) = \left(1 - \frac{\text{As}}{\text{Ac}}\right) \text{x } 100$$

where As and Ac are absorbance of sample and absorbance of control respectively. The concentrations of the peptides resulting in 50% inhibition of enzyme activity (IC_{50} values) were determined using the straight line equations of the percentage inhibitory activity against the respective logarithm of peptide concentrations.

2.6 Mechanism of DPP-IV inhibition

The peptides were subjected to enzyme inhibition kinetic experiments to determine the type of inhibition exerted on DPP-IV. The experiment was conducted according to the protocol as described above at two fixed final concentrations of the peptides (250 and 500 µM) with a variable concentration of Gly-Pro-*p*-nitroanilide (0.75 – 6 mM). The initial velocity data obtained were used to construct Lineweaver-Burk plots to determine the Michaelis constant (K_M), maximum velocity (V_{max}), inhibition binding constant (K_i) of the inhibitors and the type of inhibition for both enzymes.

2.7 Growth and maintenance of cell cultures

3T3-L1 cells were obtained at passage 39 from CELLONEX Separations and used between passage 42 - 47. Cells were maintained in DMEM supplemented with 10% (v/v) FCS and 1% (v/v) antibiotics (DMEM/FCS) at 37 °C in an atmosphere of 5% CO_2, 90% humidity in cell culture flasks until confluent, with splitting at 3 - 4 days intervals.

2.8 Cytotoxicity of 3T3-L1 cells (pre-adipocytes and adipocytes)

Undifferentiated/pre-adipocyte 3T3-L1 cells were seeded at a concentration of 0.4 X 10^4 per 90 µL in a 96 well plate and left to attach overnight at 37˚C, 5% CO_2.

For the differentiation of the 3T3-L1 cells, the pre-adipocyte cells were seeded at a concentration of 0.1 X 10^4 per 100 µL in a 96 well plate and were grown to confluence for three days. On day 4, cells were then induced to differentiate using 100 µL differentiation medium 1 (DM1) containing DMEM/FCS supplemented with final concentrations of 10 µg/mL insulin, 25 mM IBMX, 50 µM dexamethasone and 100 µM rosiglitazone. DMI was replenished every 3 days for 6 days. On day 10, DM1 was replaced with DM2 which is DMEM/FCS containing only 10 µg/mL insulin for 3 days. On day 14, the medium was replaced with DMEM/FCS only. Both undifferentiated and differentiated cells were tested for cytotoxicity by exposing the preadipocytes and the adipocytes to 10 µL peptide (50 and 100 µM, final concentration), and further incubated for 24 h at 37˚C, 5% CO_2. Cytotoxicity was then determined using the MTT assay.

2.9 Prevention of lipid-accumulation in adipocyte 3T3-L1 cells

Peptides were tested for their anti-lipid formation using differentiated 3T3-L1 cells by 2 methods: 1. Adding the peptides after full differentiation of the 3T3-L1 adipocytes (50 and 100 µM, final concentration) for 24 h. 2. Adding the peptides (50 and 100 µM, final concentration) together with differentiation media at days 4, 7 and 10. For both experiments, the effect on lipid accumulation was determined with the Oil Red O assay.

2.10 Oil Red O staining assay

Differentiated cells were treated with the peptides and incubated as described above. For the Oil Red O staining to detect oil droplets in adipocytes, cells were fixed with 2% (v/v)

formaldehyde for 30 min at 37˚C, 5% CO_2. After fixing the medium and formaldehyde were discarded and plate dried. Once dry, plates were stained with freshly diluted Oil Red O solution (0.5% Oil-Red O (w/v) in 60% isopropyl alcohol (3:2)) for 30 min. After staining of the lipid droplets, the Oil- Red O staining solution was removed and cells were rinsed with water and dried. Images of the stained lipid droplets were collected on an Olympus microscope (Olympus, Tokyo, Japan). Subsequently, the dye was extracted with 60% isopropanol and quantified by measuring the absorbance using a BioTek plate reader at 405 nm. The percentage lipid accumulation was calculated relative to the unexposed differentiated 3T3-L1 cells (100% lipid formation).

2.11 MTT assay

The potential cytotoxicity of the peptides towards both differentiated and undifferentiated 3T3-L1 cells was determined using the MTT assay. Following incubation with peptides, 10 µL of a 1 mg/mL MTT (91 µg/mL, final concentration) solution was added to each well and incubated for 3 h at 37 °C and 5% CO_2. After incubation, the medium containing MTT was removed and the plate left to dry at room temperature. The purple formazan crystals were dissolved with 50 µL 25% (v/v) dimethylsulfoxide in ethanol with shaking for approximately 10 min. The absorbance of the solution in each well was measured using a BioTek plate reader at 570 nm. Cell viability in the presence of peptides was expressed as a percentage relative to the control of either undifferentiated or differentiated cells (100% cell viability).

2.12 MGO scavenging effects of the peptides

This assay was performed as per method of Siddiqui et al. [26] with slight modifications. Briefly, 25 µL of each peptide (31.25 – 250 µM) were transferred into a 96-well fluorescence plate followed by the addition of 25 µL MGO (56 mM initial concentration). Thereafter, 50 µL of 0.1M phosphate buffer (pH 6.8) was added to a final volume of 100 µL in each well. The plate was then incubated at 37˚C for 7 days under a sterile 5% CO_2 environment. A positive control consisting of BSA (40 mg/mL initial concentration), MGO and phosphate buffer while the vehicle control consisted of the peptides and phosphate buffer. After incubation, florescence was measured at 330nm (excitation) and 420 nm (emission) wavelengths using a FLUOstar OPTIMA plate reader (BMG labtechnologies, Offenburg, Germany) and the amount of AGE formed was

expressed as percentage of florescence in the presence of the peptides and MGO relative to the positive control (MGO and BSA) (100% AGE formation).

2.13 Antioxidant assay (Oxygen radical absorbance capacity (ORAC)

The assay was conducted based on the method described by Ou et al. [27]. Briefly, 165 µL of fluorescein (0.139 nM) was added to each well of a 96 - well plate followed by 10 µL of each peptide sample (5-30 µM, final concentration) added to the wells containing fluorescein. Thereafter, 25 µL of a 0.24 mM AAPH solution was added and fluorescence was immediately measured every 60 seconds for 120 minutes, to generate 120 cycles, at an excitation and emission wavelength of 485 nm and 520 nm, respectively using a FLUOstar OPTIMA plate reader (BMG labtechnologies, Offenburg, Germany). Trolox at final concentrations of 0 – 50 µM was used to prepare a standard curve. The positive control contained fluorescein with only AAPH whereas the vehicle control contained fluorescein with ddH_2O. The area under curve was calculated and the antioxidant activity of each sample was expressed as µMTE/µM peptide.

2.14 Nitric oxide scavenging assay

A quantitative chemical assay to investigate the ability of the peptides to scavenge NO formed by the decomposition of sodium nitroprusside (SNP) [28] was undertaken. A volume of 40 µL of 5 mM SNP solution (dissolved in 0.1 M phosphate buffered saline (pH 7.4) and left to stand for 1 h in the light) was added to 10 µL of each of the peptide at a final concentration of 12.5 - 100 µM, and further incubated for 1 h at 37 ^{o}C. GSH was used as a positive control. Thereafter, 50 µL of Griess reagent (1 % sulfanilamide and 0.1% NED in 2.5% (v/v) phosphoric acid) was added. The absorbance was measured using a BioTek plate reader at 570nm. The amount NO scavenged was expressed as a percentage relative to the control containing all reagents except peptide (100% NO).

2.15 Statistical analysis

Values are presented as mean ± SD of two independent experiments done in triplicates and the data were analyzed by using a statistical software package (SPSS for Windows, version 18, IBM Corporation, NY, USA) using Tukey's-HSD multiple range *post-hoc* test. Values were considered significantly different at $p < 0.05$.

3. Results

In order to investigate the potential of the 3 previously reported α-glucosidase inhibitory peptides to also inhibit DPP-IV, the peptides were initially subjected to molecular docking studies to determine their binding free energies towards DPP-IV in comparison to a standard inhibitory peptide (diprotin A; IPI). Interestingly, all 3 peptides had binding free energies $\leq$ - 7.0 kcal/mol which was lower than the observed -6.0 kcal/mol of diprotin A (Table 1). The binding free energy was in the order of PFP < YPG < YPL < diprotin A. Subsequently, at these binding free energies, PFP interacted with the enzyme close to the active site but with no hydrogen bond interaction while YPL interacted at a site distant from the active site with a single hydrogen bond interaction (Fig. 1). Both YPG and diprotin A binds the human DPP-IV at the active site with 1 and 2 hydrogen bond interactions, respectively (Fig. 1). The hydrogen bond interactions occur between the amino acid residues at positions 1 and 3 (L3 and Y1 for YPL and YPG respectively and I1 and I3 for diprotin A) and various residues on the enzyme with a range of bond distances from 2.078 Å to 2.323 Å (Table 1). Noteworthy among the residues on the enzyme is W629 which formed hydrogen bond with I1 on diprotin A.

Table 1. Docking results and binding free energy (kcal/mol) of the tripeptides and diprotin A with the human dipeptidyl peptidase IV

Peptide ligand	Binding energy (kcal/mol)	Number of hydrogen bonds	Interacting residue of the peptide	Interacting residue of the DPP IV	Hydrogen bond distance (Å)
PFP	-7.6	0	-	-	-
YPL	-7.0	1	L3 (N-H)	K122 (C=O)	2.252
YPG	-7.4	1	Y1 (OH)	Q553 (*NH_2)	2.078
IPI (Diprotin A)	-6.0	2	I1 (NH_2)	W629 (C=O)	2.297
			I3 (C=O)	K554 (*NH_2)	2.323

The functional groups involved in the hydrogen bond formation are indicated in parenthesis next to the respective amino acid residues. NH_2 refers to the free amino group at the N-terminal of the while *NH_2 refer to the amino groups on the side chain of glutamine and lysine.

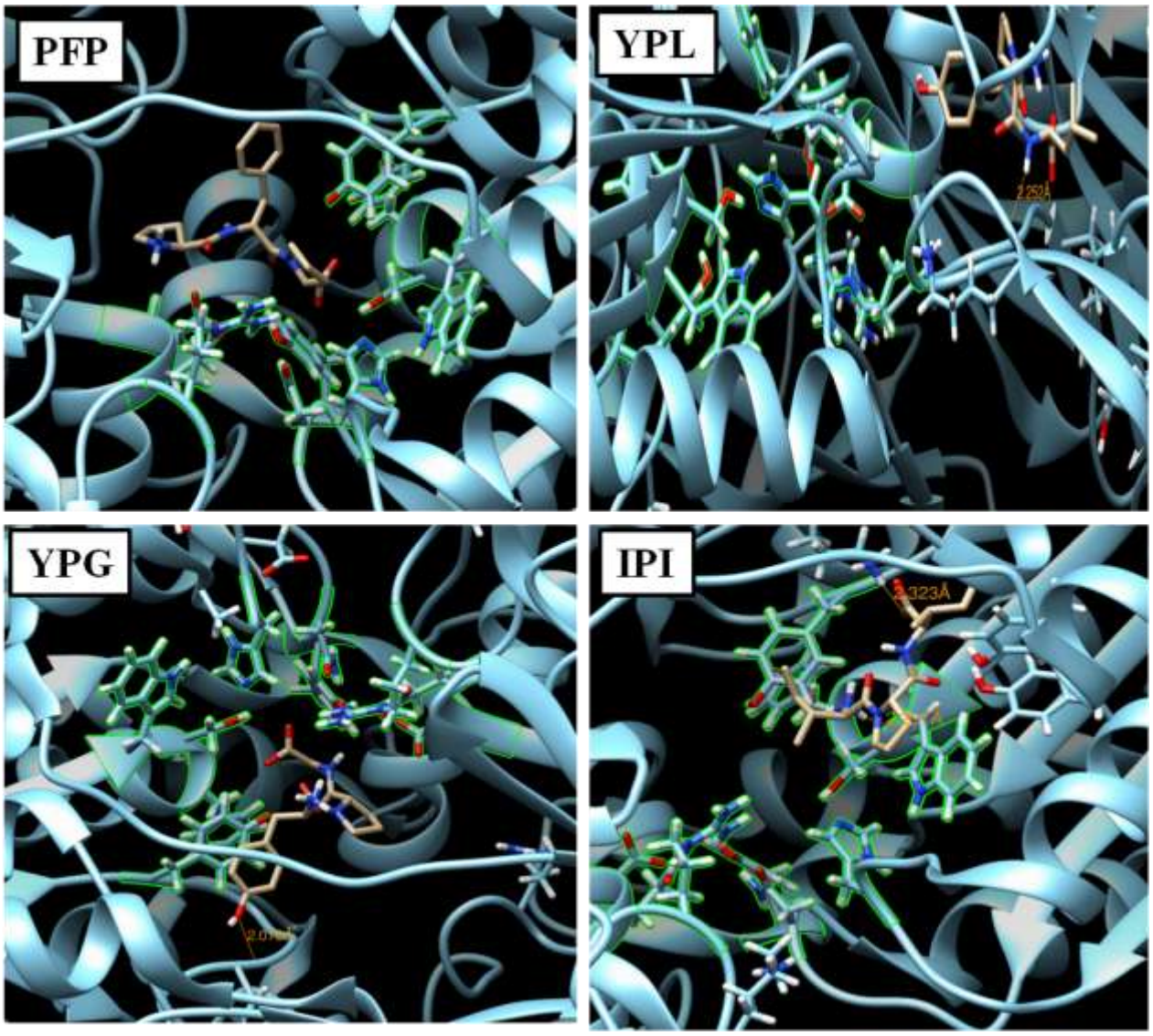

Fig. 1. The mode of interaction between PFP, YPL, YPG and IPI with the human DPP-IV. The orange line represents the hydrogen bonds with the respective bond distance while the green area indicated the active site residues. The binding site has been zoomed out for each peptide-DPP-IV interaction and presented.

For comparative and validation purposes, the *in vitro* α-glucosidase inhibitory activities of the peptides were initially investigated which revealed that PFP had significantly lower IC_{50} values for α-glucosidase inhibition (IC_{50} = 329.20 ± 46.95 µM) than YPL and YPG (Table 2). To confirm the *in silico* results, the *in vitro* DPP-IV inhibitory potential of each peptide was determined. A dose-dependent pattern (not shown) was observed with IC_{50} values several fold higher than that of diprotin A (IC_{50} = 3.52 ± 1.40 µM) (Table 2) with YPG having significantly (p

< 0.05) lower IC_{50} values for DPP-IV inhibition (IC_{50} = 173.96 ± 11.32 µM) than YPL (IC_{50} = 364.62 ± 46.35 µM) and PFP (IC_{50} = 1389.14 ± 550.32 µM). Enzyme kinetic studies revealed that the 3 peptides were uncompetitive inhibitors of DPP-IV with computed inhibition binding constants (Ki) of 154.28, 48.63 and 0.016 µM for PFP, YPL and YPG inhibitions, respectively (Fig. 2A-C). In contrast, diprotin A was determined to be a competitive inhibitor of DPP-IV with a Ki of 0.00054 µM (Fig. 2D).

Table 2: IC_{50} values for α-glucosidase and DPP-IV inhibition by the tripeptides

Peptide/standard		IC_{50} (µM)	
	Reported α-glucosidase inhibition	Validated α-glucosidase inhibition	DPP-IV inhibition
PFP	8.62	329.20 ± 46.95[a]	1389.14 ± 550.32[c]
YPL	3900	2581.30 ± 335.28[b]	364.62 ± 46.35[c]
YPG	5000	10249.94 ± 407.74[d]	173.96 ± 11.32[b]
Diprotin A	-	-	3.52 ± 1.40[a]
Acarbose	-	1722.97 ± 655.80[c]	-

Data are expressed as mean ± SD of two independent experiments done in triplicates. [a-b]Values with different subscript letters along a column are significantly different from each other (Tukey's-HSD multiple range post hoc test, $p < 0.05$).

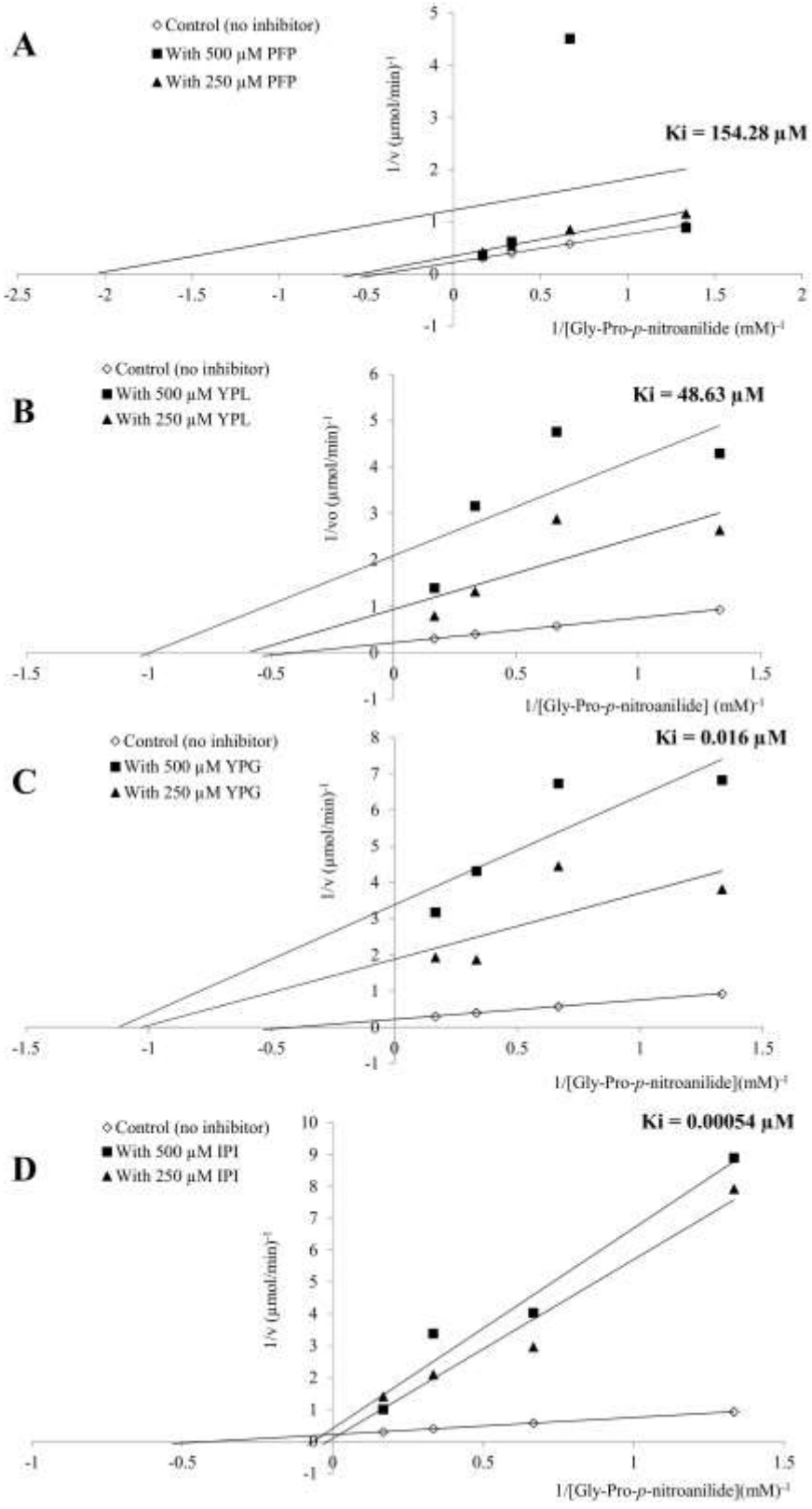

Fig. 2. Lineweaver-Burke's plots of DPP-IV catalysed reactions in the presence of PFP, YPL, YPG and IPI. Each data point represents a mean of two independent experiments done in triplicates

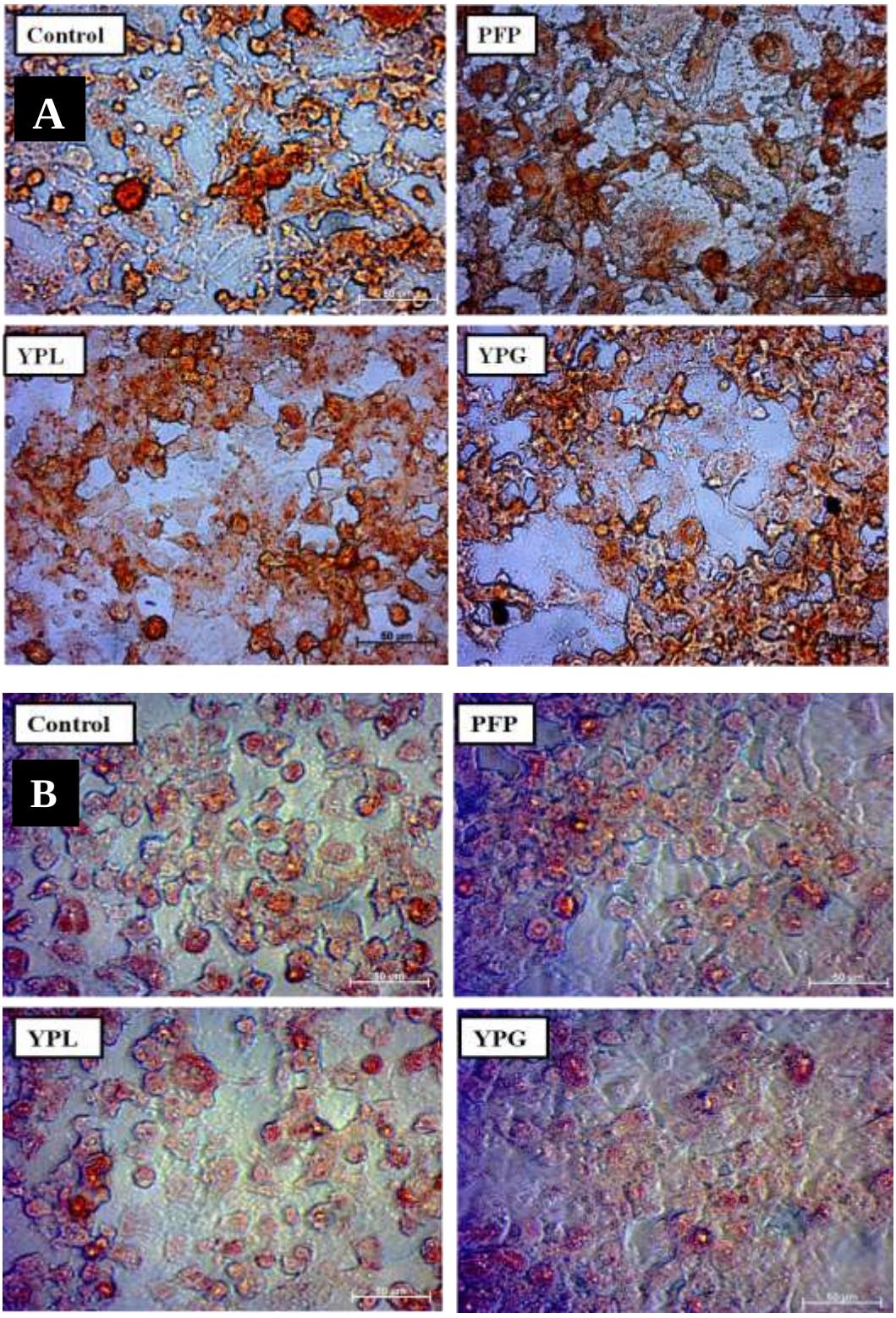

Fig. 3. Representative micrographs for lipid accumulation based on Oil Red O staining of 3T3-L1 differentiated adipocytes in the presence of 100 µM PFP, YPL and YPG after (**A**) and during (**B**) the differentiation process. The cells were photographed at magnification x40.

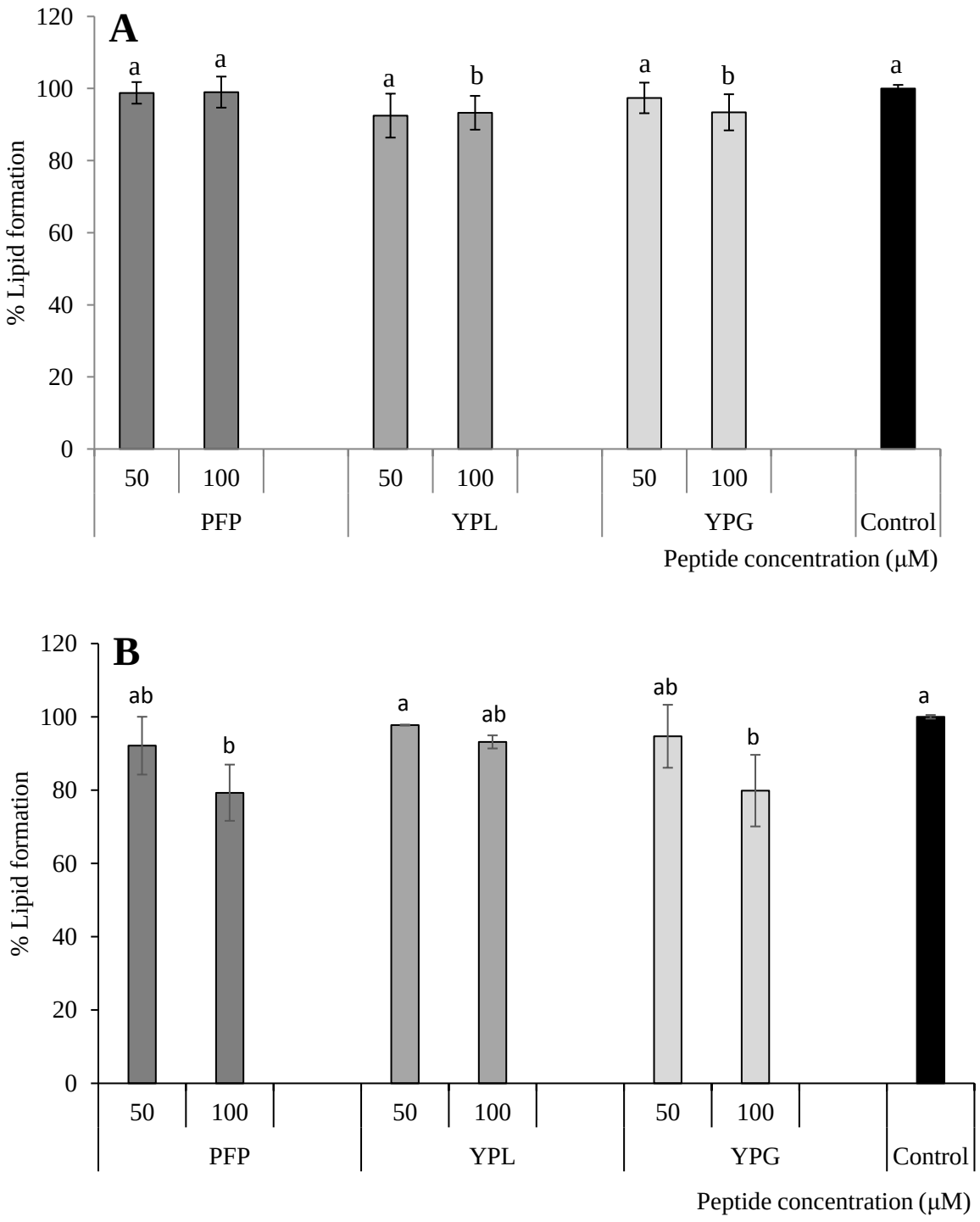

Fig. 4. Quantitative analysis of lipid accumulation in Oil Red O stained differentiated 3T3-L1 adipocytes in the presence of PFP, YPL and YPG after (**A**) and during (**B**) the differentiation process. Lipid accumulation in the presence of the peptides was expressed as a percentage of the vehicle control. Data are expressed as mean ± SD of two independent experiments done in triplicates. $^{a-b}$Values with different subscript letters over the bars are significantly different from each other (Tukey's-HSD multiple range post hoc test, $p < 0.05$).

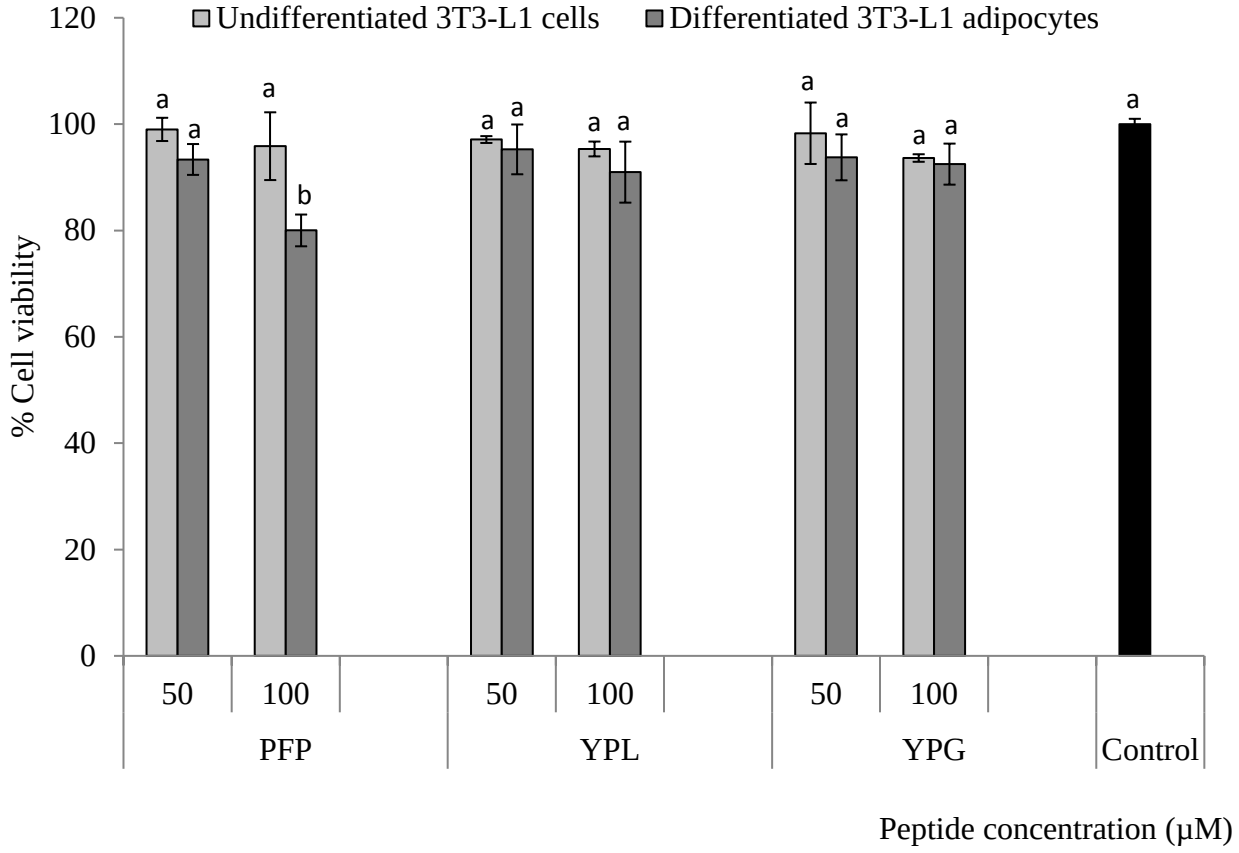

Fig. 5. The cytotoxic effects of PFP, YPL and YPG on undifferentiated 3T3-L1 cells and differentiated 3T3-L1 adipocytes. Cell viability in the presence of the peptides was expressed as a percentage of the vehicle control. Data are expressed as mean ± SD of two independent experiments done in triplicates. [a-b]Values with different subscript letters over the bars are significantly different from each other (Tukey's-HSD multiple range post hoc test, $p < 0.05$)

The differentiation of 3T3-L1 cells to adipocytes was successful with lipid droplet formation and positive Oil Red O staining (Fig. 3). The results indicated that, all the peptides at 100 µM did not clearly reduce lipid droplets in the differentiated 3T3-L1 adipocytes when added for 48 hours after the differentiation process (Fig. 3A). Subsequently, the ability of the peptides to prevent the lipid formation was also investigated where the 3T3-L1 cells were exposed to the peptides for 6 days during the differentiation process. Following exposure to the peptides after differentiation, the quantitative analysis revealed a significant reduction ($p < 0.05$) in the percentage lipid formation for the 3T3-L1 cells exposed to 100 µM of YPL and YPG (Fig. 4A). However, when the 3T3-L1 cells were exposed to the peptides during the differentiation, there was a significant decrease ($p < 0.05$) in the lipid accumulation for all the peptides at 100 µM and the reduction

was approximately 20% for PFP and YPG but 7% for YPL (Fig. 4B). The cytotoxicity effects of the peptides on the viability of undifferentiated and differentiated 3T3-L1 cells were determined. At a concentration of 50 and 100 µM, all peptides demonstrated no cytotoxicity towards the undifferentiated 3T3-L1 cells because the cell viability was not significantly ($p > 0.05$) affected by any of the peptides (Fig. 5). However, at 100 µM, exposure to PFP resulted in a significant ($p < 0.05$) decrease in cell viability of the differentiated 3T3-L1 adipocytes while YPL and YPG at 50 and 100 µM adversely affected the cellular viability (Fig. 5).

Fig. 6 presents the interactions of the peptides with MGO forming AGEs. At 31.25 – 250 µM, both PFP and YPL reacted with MGO to form a concentration dependent increase of 22.75 – 44.82 and 23.20 – 42.84 % in AGE formation, respectively. No dose dependent increase in AGE formation was observed for YPG and GSH.

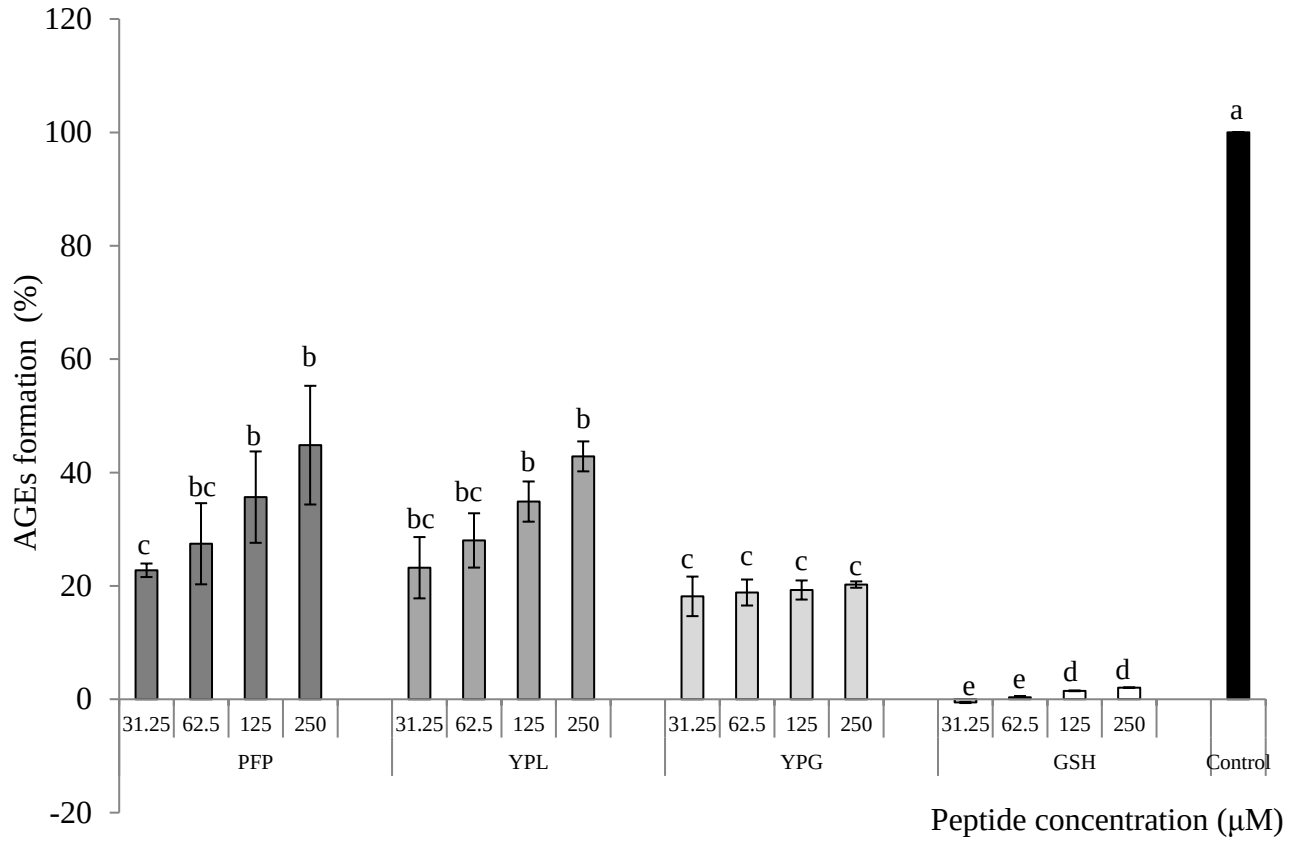

Fig. 6. Interaction of different concentrations of PFP, YPL and YPG with MGO to form AGEs. Data are expressed as mean ± SD of three independent experiments done in triplicates. [a-e]Values with different subscript letters over the bars are significantly different from each other (Tukey's-HSD multiple range post hoc test, $p < 0.05$)

The ability of the peptides to scavenge AAPH generated radicals was then assessed with the ORAC assay. PFP showed no antioxidant activity, while for YPL and YPG, a dose dependent increase in antioxidant activity (Fig. 7) was observed, although the difference between these peptides was not significant ($p > 0.05$). At 5 and 10 μM, YPG had higher antioxidant activity than YPL and GSH, while at 20-30 μM, the difference in antioxidant activity between YPL, YPG and GSH was not significant ($p > 0.05$). The ability of the peptides to scavenge NO thereby reducing RNS was then determined. PFP showed very low NO scavenging activity while both YPG and GSH showed a dosage related increase in activity between 25 and 50 μM ($p > 0.05$). At 50 and 100 μM, the NO scavenging activity of YPG and GSH was similar.

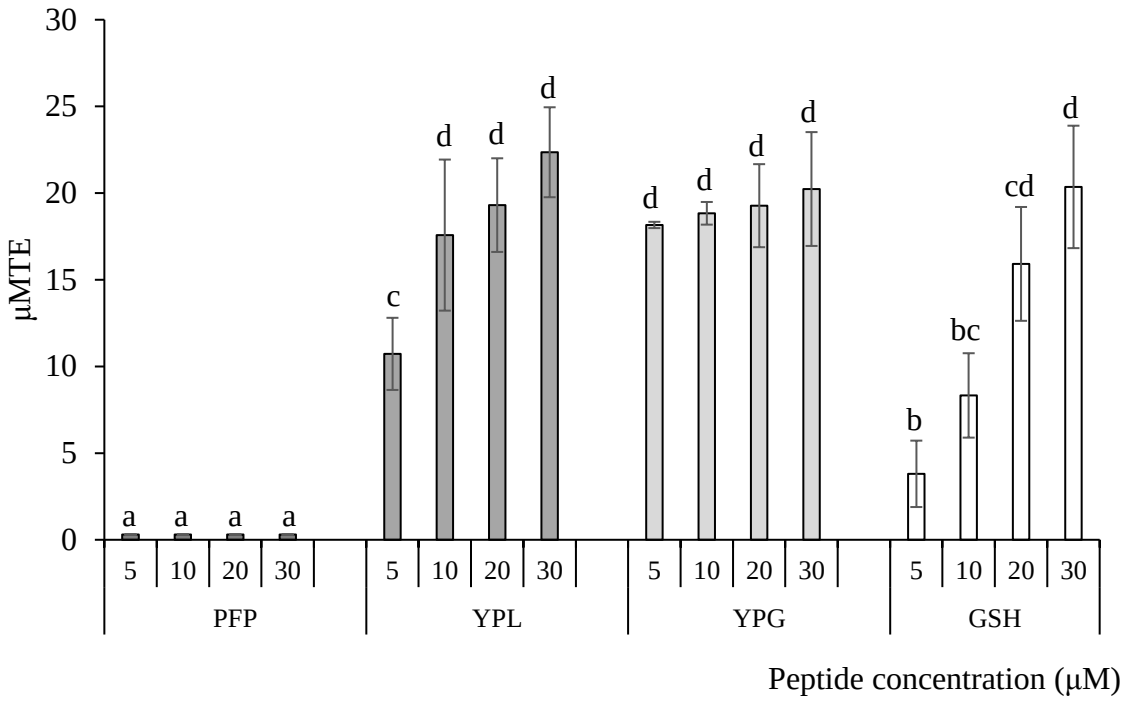

Fig. 7. Oxygen radical absorbance capacity (ORAC) based antioxidant activity of different concentrations of PFP, YPL, YPG and GSH. Data are expressed as mean ± SD of two independent experiments done in triplicates. [a-c]Values with different subscript letters over the bars are significantly different from each other (Tukey's-HSD multiple range post hoc test, $p < 0.05$)

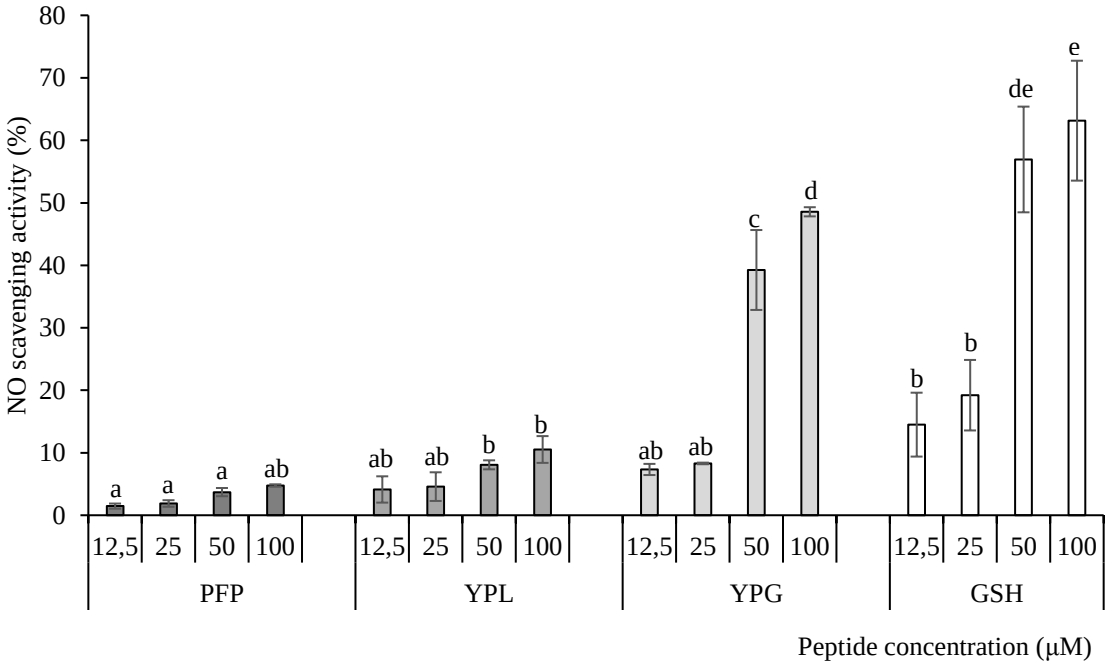

Fig. 8. Nitric oxide (NO) scavenging activity of PFP, YPL, YPG and GSH. The amount of NO scavenged in the presence of the peptides was expressed as a percentage of a control containing all reagents except the peptides. Data are expressed as mean ± SD of two independent experiments done in triplicates. [a-d]Values with different subscript letters over the bars are significantly different from each other (Tukey's-HSD multiple range post hoc test, $p < 0.05$)

4. Discussion

T2DM is a complex multifaceted disease that affects a variety of metabolic systems and organs which makes the development of antidiabetic drugs with multiple targets to be of utmost pharmaceutical importance. The peptides PFP, YPL and YPG were previously reported to exhibit antidiabetic effects via α-glucosidase inhibition [11, 21, 22]. The present study demonstrated that the three peptides have multiple antidiabetic effects but YPG has the greatest pharmaceutical potential as antidiabetic candidate.

The observed binding of the peptides to the DPP-IV with a free energy of $\leq$ - 7.0 kcal/mol comparable to that of diprotin A indicates that the peptides may interact with the enzyme to form peptide-DPP-IV complexes suggesting possible DPP-IV inhibitory effects. The binding energy values compared favourably with the -6.0 to - 9.0 kcal/mol observed for 95% of tripeptides studied by Nongonierma et al. [29]. Unlike the study of Nongonierma et al. [30] which was restricted to competitive type of interaction, the present study did not include any bias towards a

particular type of inhibition which allows a more precise and unrestricted prediction of the binding pattern of the peptides. This led to the observation that PFP and YPG had a competitive-like type of interaction while PFP had the best binding affinity without a hydrogen bond while YPG formed a single hydrogen bond interaction. It was noted that the active site residues of the human DPP-IV used in this study comprise of R125, Q205, Q206, Y547, W629, S630, Y631, Y662, N710 and H740 but none of these residues was involved in the hydrogen bond formation with YPG suggesting that other kind of interactions might be responsible for trapping YPG around the active site of the enzyme. Indeed, hydrophobic interactions between tyrosine residue and the hydrophobic S1 pocket of DPP-IV were shown to be critical for the binding of competitive DPP-IV inhibitory peptides to the active site of the enzyme [29, 31].

Prior to the *in vitro* validation of the above molecular docking experiment, it was important to also validate the reported α-glucosidase inhibitory activities of the three peptides. Highly varied IC_{50} values were observed between the previous studies [21, 22] and our present investigation using the same assay method. The IC_{50} was 38.19 fold higher, 0.66 fold lower and 2.04 fold higher for PFP, YPL and YPG respectively. This clearly demonstrates the importance of validation of reported activity before definite conclusions are made about the precise activity of α-glucosidase inhibitory peptides. The high variation of the IC_{50} value of acarbose across laboratories from high millimolar to low micromolar values further supports this assertion. Upon confirming the α-glucosidase inhibitory activity of the peptides, the *in vitro* DPP-IV inhibitory activities were then determined in order to validate the *in silico* findings. In patients with T2DM, inhibition of DPP-IV increases the half-lives of incretins, increases insulin secretion and decrease blood glucose levels [13]. However, in contrast to molecular docking analysis which identified PFP as the best candidate peptide, the *in vitro* experiments revealed YPG to be the best DPP-IV inhibitory peptide. In fact, YPG was more potent as DPP-IV inhibitor than a number of other tripeptides WWW, LPL, LQP, IQP and VGL reported with DPP-IV inhibitory activity [29]. To the best of our knowledge, apart from IPI, IPM, LPQ and VPL [29, 30, 32, 33], no other tripeptide with higher DPP-IV inhibitory than YPG could be found after searching the entire BIOPEP database (http://www.uwm.edu.pl/biochemia/index.php/en/biopep). The IPI is a known DPP-IV inhibitory peptide commonly used as positive control [29, 30]. However, Rahfeld et al. [34] reported that an apparent competitive inhibition of DPP-IV by the IPI is an interesting kinetic artefact. Subsequently, several studies have confirmed this finding for tripeptides that

showed competitive and mixed-type inhibition [35, 36]. Interestingly, the competitive inhibition of DPP-IV by IPI was also confirmed in the present study but in contrast, the inhibition of DPP-IV by the peptides, PFP, YPL and YPG was found to be uncompetitive. Therefore, hydrolysis may not occur because this type of inhibition is the result of the peptides binding at a site separate from the active site. Moreover, the uncompetitive inhibition pattern also suggests that PFP, YPL and YPG interacted with the DPP-IV - Gly-Pro-*p*-nitroanilide complex. This observation also contradicts the molecular docking experiment where YPG and PFP showed competitive type of interaction, but it is known that molecular docking analysis does not always correlate with *in vitro* experiments [37]. A poor correlation was also reported between molecular docking of peptides and the *in vitro* kinetic experiments which was identified to be due to confounding factors such as peptide molecular mass and the *in vitro* reaction environments [30]. However, diprotin A consistently demonstrated competitive inhibition pattern. Further in-depth studies to elucidate the observed differences between *in silico* and *in vitro* findings may provide insight into the reaction mechanism of DPP-IV inhibitory peptides. In spite of these anomalies, it was interesting to note that kinetic analyses also showed that YPG had the lowest Ki value compared to PFP and YPL.

Lipid accumulation is an important metabolic consequence of T2DM and plays a vital role in the development of secondary macrovascular complications associated with the disease. Furthermore, adipocyte differentiation is important because thiazolidinediones (a class of antidiabetic drugs) are pharmacological ligands for the nuclear receptor, peroxisome-proliferator-activated receptor gamma (PPARϒ). The latter plays critical roles in the process of adipocyte differentiation [38]. Sabbu et al. [39] evaluated the effects of amino alcohol derivatives and thiazolidine hybrids on the differentiation of 3T3-L1 cells. Findings were that several of these derivatives were not cytotoxic and inhibited adipocyte differentiation. The mechanism of action of the most active derivative was via the suppression of adipocyte specific genes including PPARγ, C/EBPα, FAS and AP2. Likewise, the present study found that PFP and YPG inhibited adipocyte differentiation although the effect observed for PFP may be due to the cytotoxicity of this peptide. The percentage inhibition was comparable to several of the amino alcohol derivatives and thiazolidine hybrids evaluated by Sabbu et al. [39]. Other peptides such as GEY and GYG at a concentration of 250 µM [40] and DIIADDEPLT (10 µM) [41] were shown to suppress lipid droplets in differentiated adipocytes suggesting that other peptide variables, apart

from concentration, such as direct inhibitory effects on adipocyte differentiation genes or an effect on lipid droplet formation. 3T3-L1 cells express DPP-IV which becomes liberated after differentiation [42] and therefore the observed effect of YPG on the DPP-IV activity and lipid accumulation in 3T3-L1 cells could be intricately interconnected. For therapeutic purposes, multifunctional peptides must be non-toxic on normal mammalian cells and interestingly, the MTT assay revealed that the peptides have no effect on the normal mammalian cell viability indicating lack of cytotoxicity.

Accumulation of MGO is a detrimental consequence of T2DM and an important biological process involved in diabetic pathogenesis [18]. MGO is a highly reactive intermediate carbonyl compound which reacts with the free amine groups of relevant tissue macromolecules leading to the formation of AGEs [43]. AGE formation, causes protein dysfunction and MGO derived AGEs can bind to the receptor for AGEs (RAGE) and this can activate an inflammatory response which is a clinical characteristic of T2DM. Therefore, effective reduction of MGO levels would reduce AGE formation and consequently inflammation. Indeed, the reduction of MGO is currently considered as a promising glucose independent strategy for retarding diabetic complications [19]. Like proteins, MGO can also bind peptides forming small AGE products. Although, this can compromise the activity of the peptides, a beneficial effect is that small peptides can act as MGO scavengers thereby sparing endogenous relevant macromolecules from the non-enzymatic attack by the highly reactive carbonyl group of MGO and this will enable the macromolecules to proceed with the normal cellular functions. Both PFP and YPL showed a dose dependent ability to scavenge MGO, while some scavenging effects were observed for YPG but not for GSH, suggesting that proline might be important for the observed MGO scavenging effects. AGE-RAGE interaction results in an inflammatory response involving an increase of NADPH oxidase activity, the activation of Nf-κβ leading to the upregulation of iNOS and increased formation of NO. Reactive oxygen species react with NO forming peroxynitrite which causes oxidative protein damage. Thus, identified targets to inhibit protein damage and dysfunction are to lower MGO levels and scavenge ROS and/or NO. The antioxidant activity of YPL and YPG was comparable to GSH, while PFP had no antioxidant activity. In addition, YPG and GSH effectively scavenged NO while the effect of PFP and YPL was low suggesting that glycine may be relevant for this activity. Based on all these observations, YPG seems to have the

best protective effects against the above mentioned identified targets for inhibiting protein damage.

In conclusion, three previously reported α-glucosidase inhibitory peptides, PFP, YPL and YPG have demonstrated uncompetitive DPP-IV inhibitory activity. Additional beneficial properties of these peptides were the ability to reduce adipocyte differentiation and lipid accumulation as well as scavenge MGO, ROS and NO. Although the α-glucosidase activity of YPG was the lowest among the peptides evaluated, its DPP IV inhibitory activity was the highest. Furthermore, this peptide was not cytotoxic, inhibited adipocyte differentiation and had antioxidant properties comparable to GSH. Therefore, YPG was identified as the best candidate peptide that warrants further studies for potential application as a multifunctional antidiabetic agent.

Acknowledgement

We acknowledge the National Research Foundation of South Africa and the University of Pretoria for the financial support. The first author also acknowledges the University of Pretoria for the award of a postdoctoral fellowship position in Biochemistry and Ahmadu Bello University, Zaria, Nigeria for the award of a study fellowship.

References

[1] M. Brownlee, Nature. 414 (2001) 813–820.

[2] H. Arimochi, Y. Sasaki, A. Kitamura, K. Yasutomo, Sci. Rep. 6 (2016) 26791.

[3] R.A De Fronzo, C. L. Triplitt, M. Abdul-Ghani, E. Cersosimo, Diabetes Spectrum 27 (2014) 100-112.

[4] S. E. Inzucchi, R. M. Bergenstal, J. B. Buse, M. Diamant, E. Ferrannini, M. Nauck, A. L. Peters, A. Tsapas, R. Wender, D. R. Matthews, Diabetologia 58 (2015) 429-442.

[5] R. J. FitzGerald, B. A Murray, Int. J. Dairy Technol. 59 (2006) 118.

[6] S. Wang, X. Zeng, Q. Yang, S. Qiao, Int. J. Mol. Sci. 17 (2016), 603.

[7] H. G. Byun, J. K. Lee, H. G. Park, J. K. Jeon, S. K. Kim, Process Biochem. 44 (2009) 842-846.

[8] T. Lafarga, P. O. Connor, M. Hayes, Peptides. 59 (2014) 53-62.

[9] C. M. Yin, J. H. Wong, J. Xia, T. B. Ng, Curr. Prot. Pept. Sci. 14 (2013) 492–503.

[10] Y. W. Park, M. S. Nam, Korean J. Food Sci. Animal Res. 35 (2015), 831-840.

[11] M. A. Ibrahim, M. J. Bester, A. W. H. Neitz, A. R. M. Gaspar, Chem. Biol. Drug Des. 91 (2) (2018) 370 -379.

[12] H. Lee, H. J. Lee, H. J. Suh, Nutr. Res. 31 (2011) 937–943.

[13] I. M. Lacroix, E. C. Li-chan, Trends Food Sci. Technol. 54 (2016) 1-16.

[14] F. Giacco, M. Brownlee, Circ. Res. 107 (2010) 1058 – 1070.

[15] J. H. Kim, S. J. Park, B. Kim, Y. G. Choe, D. S. Lee, PLoS ONE. 12 (10) (2017) e0185764.

[16] P. E. Scherer, Diabetes. 55 (6) (2006) 1537-1545.

[17] D. Pitocco, F. Zaccardi, E. Di Stasio, F. Romitelli, S. A. Santini, C. Zuppi, G. Ghirlanda, The Review of Diabetic Studies. 7 (2010) 15-25.

[18] N. J. R. Blackburn, B. Vulesevic, B. McNeill, C. E. Cimenci, A. Ahmadi, M. Gonzalez-Gomez, A. Ostojic, Z. Zhong, M. Brownlee, P. Beisswenger, R. W. Milne, E. J. Suuronen, Basic Res. Cardiol. (2017) 112:57 DOI 10.1007/s00395-017-0646-x

[19] A. Moraru, J. Wiederstein, D. Pfaff, T. Fleming, A. K. Miller, P. Nawroth, A. A. Teleman, Cell Metab. 27(4) (2018) 926-934.

[20] O. Trott, A. J. Olson, J Comput. Chem. 31 (2010) 455–461.

[21] T. Matsui, T. Oki, Y. Osajima, Z. Naturforsch 54c (1999) 259-263.

[22] M. Kang, S. Yi, J. Lee, Mycology. 41(3) (2013) 149-154.

[23] M. A. Ibrahim, N. Koorbanally, M. S. Islam, Acta Pharm. 64 (2014) 311-324.

[24] L. J. Shai, P. Masoko, M. P. Mokgotho, S. P. Magano, A. M. Mogale, N. Boaduo, J. N. Eloff, South Afr. J. Bot. 76 (2010) 465–470.

[25] B. Konrad, A. Dabrowski, M. Szoltysik, P. Marta, Z. Aleksandra, C. Jozefa, Int. J. Pept. Res. Ther. 20 (2014) 483-491.

[26] M. A. Siddiqui, S. Rasheed, Q. Saquib, A. A. Al-Khedhairy, M. S. Al-Said, J. Musarrat, M. I. Choudhary, BMC Complement. Altern. Med. 16 (2016) 276.

[27] B. Ou, D. Huang, M. Hampsch-Woodill, J. A. Flanagan, E. K. Deemer, J. Agric. Food Chem. 50 (2002) 3122–3128.

[28] D. Giustarini, R. Rossi, A. Milzani, I. Dalle-Donne, Methods Enzymol. 440 (2008) 361–380.

[29] A. B. Nongonierma, R. J. FitzGerald, Peptides. 79 (2016) 1-7.

[30] A. B. Nongonierma, C. Mooney, D. C. Shields, R. J. FitzGerald, Peptides. 54 (2014) 43-51.

[31] M. Engel, T. Hoffmann, S. Manhart, U. Heiser, S. Chambre, R. Huber, H. U. Demuth, W. Bode, J. Mol. Biol. 355 (2006) 768–783.

[32] H. Uenishi, T. Kabuki, Y. Seto, A. Serizawa, H. Nakajima, Int. Dairy J. 22 (2012) 24-30.

[33] S. Maruyama, T. Ohmori, T. Nakagami, Biosci. Biotech. Biochem., 60 (1996) 358-359.

[34] J. Rahfeld, M. Schierhorn, B. Hartrodt, K. Neubert, J. Heins, Biochim. Biophys. Acta. 1076 (1991) 314 – 316.

[35] T. Hatanaka, K. Kawakami, M. Uraji, J. Enz. Inh. Med. Chem. 29 (2014) 823 – 828.

[36] A. B. Nongonierma, L. Dellafiora, S. Paolella, G. Galaverna, P. Cozzini, R. J. FitzGerald, Front. Endocrinol. 9 (2018) 329.

[37] C. Y. Chen, Trends Pharmacol. Sci. 36(2) (2015) 78-95.

[38] T. Tzeng, C. J. Chang, I. Liu, Phytother. Res. 28 (2014) 187–192.

[39] S. Sabbu, A. Srivastava, P. Yadav, S. Varshney, R. Choudhary, V. M. Balaramnavar, A. N. T. Gaikwad, Eur. J. Med. Chem. 143 (2018) 780-791.

[40] B. K. Han, H. J. Lee, H. Lee, H. J. Suh, Y. Park, J. Sci. Food Agric. 96 (2016) 116–121

[41] P. Reckziegel, W. T. Festuccia, L. R. G. Britto, K. L. L. Jang, C. M. Romão, J. C. Heimann, M. V. Fogaça, N. S. Rodrigues, N. R. Silva, F. S. Guimarães, R. A. S. Eichler, A. Gupta, I. Gomes, L. A. Devi, A. S. Heimann, E. S. Ferro, Sci Rep. 7(1) (2017) 14781.

[42] P. ZilleBen, J. Celner, A. Kretschmann, A. Pfeifer, K. Racke, P. Mayer, Sci. Rep. 6 (2016) 23074.

[43] S. Y. Goh, M. E. Cooper, J. Clin. Endocrinol. Metab. 93(4) (2008) 1143-1152.